JETIR.ORG ISSN: 2349-5162 | ESTD Year : 2014 | Monthly Issue
JOURNAL OF EMERGING TECHNOLOGIES AND INNOVATIVE RESEARCH (JETIR)
An International Scholarly Open Access, Peer-reviewed, Refereed Journal

Green Corrosion Inhibitor for Mild Steel in Phosphoric Acid: Psidium Guajava Leaf Extract

Dr. Kailash Chand
(Co-guide)
Department of Chemistry
S.P.C Government College,
Ajmer Rajasthan

Sharwan Kumar Devanda
(Research Scholar)
S.P.C. Government College Ajmer

Email :- sharwankumardevanda@gmail.com

Abstract:-

Weight loss, potentiodynamic polarization, and electrochemical impedance spectroscopy techniques were used to evaluate In a 1M phosphoric acid media, the adsorption and corrosion prevention capabilities of alcoholic Psidium guajava (guava) leaf extract on mild steel were investigated. According to the research, the inhibitory efficacy increases with increasing inhibitor concentration up to 800 ppm, then drops slightly at 1200 ppm. Both the Langmuir and Temkin adsorption isotherm equations are obeyed by the adsorption. Thermodynamic and kinetic parameters were calculated and discussed. It was revealed that the adsorption was of a full nature, with chemisorption dominating. According to potentiodynamic polarisation tests, the inhibitor functioned like a mixed-type inhibitor.

Keywords: EIS, Tafel, mild steel, corrosion, adsorption

1. INTRODUCTION :

One of the most essential metals in industry is mild steel. In some sectors, the use of corrosive chemicals is unavoidable, which could result in metal disintegration. At the industrial level, several approaches such as corrosion prevention coatings, cathodic protection, anodic protection, and inhibitors are available to protect the metal surface from the harsh environmentAmong the numerous corrosion prevention techniques, the use of corrosion

inhibitors is widely chosen because the amount of inhibitor required to achieve a successful outcome is usually less [1].Various synthetic organic and inorganic compounds have been investigated as mild steel corrosion inhibitors in various aqueous conditions [2].Various synthetic organic and inorganic compounds have been investigated as mild steel corrosion inhibitors in various aqueous conditions [2]. Because synthetic inhibitors are harmful in nature, natural substances with a strong affinity for metal surfaces are being investigated [3]. Many synthetic compounds that are environmentally friendly have been investigated as alternatives to harmful organic molecules [4-20. and antihistamines Plant-based corrosion inhibitors are favored because they are commonly available, affordable, and have the added benefit of being environmentally friendly. Many research [21-33]. Anupama and Abraham [21] .Their findings revealed that as the inhibitor concentration was increased, the corrosion current (Icorr) decreased dramatically, and the adsorption followed the Frumkin isotherm [21]. In fertiliser factories, phosphoric acid is commonly employed. Phosphoric acid produced by the wet procedure is very corrosive, depending on the proportion of impurities [33]. Corrosion inhibitors for mild steel in phosphoric acid medium have been reported in just a few studies [2, 16, 18-20, 28, 33,34]. The corrosion inhibitory properties of phenacyldimethylsulfonium bromide and triazoles have been used to inhibit, In the presence of phosphoric acid, mild steel corrosion occurs [19, 20]. On the other hand, a green corrosion inhibitor for mild steel in phosphoric acid medium has received significantly less attention [2, 33]. In a 1M H3PO4 solution,apricot juice was found to have good corrosion prevention effects on mild steel [28]. The corrosion inhibition efficacy of Zenthoxylum alatum has been investigated in various concentrations of phosphoric acid [33]. Weight loss measurements, potentiodynamic polarisation, and electrochemical impedance spectroscopy measurements (EIS) studies were used to investigate the corrosion inhibition capabilities. To investigate the effect of the inhibitor on the mild steel surface, The surface of the samples was examined using scanning electron microscopy (SEM).To describe the interaction between metal and plant extract, Fourier transform infrared spectroscopy (FTIR) was used to Examine mild steel that has been treated with guava leaf extract.

2. EXPERIMENTAL

2.1Preparation of plant extract

Powdered dried guava leaves (100 g) were soaked in 500 mL methanol for 24 hours. After that, the mixture was filtered, and the filtrate was refluxed at 50°C for 4 hours. Using a vacuum evaporation equipment, the liquid obtained was concentrated and used in the investigations.

2.2. Weight-loss studies

The weight loss studies were carried out by immersing pre-weighed mild steel coupons with a diameter of 10 mm and a thickness of 5 mm in a solution of phosphoric acid. Different inhibitor dosages and temperatures were used in the weight loss testing. Before the weight loss investigations, the mild steel coins were polished with 200, 400, 600, 800, 1000, and 2000 grades of SiC and paper, then washed with acetone and double distilled water. The washed coins were dried and weighed before being put in the test sample. The effect of inhibitor concentration was investigated by immersing the coins in different inhibitor concentrations for 60 minutes and 15 minutes.

2.3. Electrochemistry experiments

Parstat 2263 potentiostat was used for the electrochemical studies (Princeton applied research, USA). The measurements were taken with a three-electrode cell. A mild steel working electrode was used in the electrochemical studies. The working electrode was made from a mild steel rod with a diameter of 5 mm and a length of 15 mm, which was sealed within a Teflon tube with a hole of 7 mm. The reference electrode was silver-silver chloride (Ag/AgCl), while the counter electrode was platinum gauze. For electrolyte preparation, Millipore water was employed. The working electrode was polished with various degrees of sand paper, rinsed, then polished again with various grades of alumina powder prior to each experiment. For potentiodynamic polarisation and EIS studies, a one-hour stabilisation interval was allowed. Tafel runs were carried out in the -250 mV to +250 mV potential range relative to the corrosion potential. The Tafel run was performed at a scan rate of 1 mVs-1. The corrosion current densities and other Tafel fit parameters were calculated using the Tafel extrapolation method. The EIS experiments were carried out in a frequency range of 100 kHz to 0.1 Hz, with a potential amplitude of 10 mV rms. The impedance tests were carried out with the circuit open (OCP). The electrochemical tests were carried out at room temperature with phosphoric acid and extract quantities varying.

2.4. Surface examination

The surface study of the steel coupons was carried out by immersing the cleaned sample in a 1 M phosphoric acid solution with and without an 800 ppm inhibitor for 6 hours before washing and drying it. The surface analysis was performed on the coupons that had been created in this manner. Coin surface analysis was investigated.

Scanning electron microscope was used.

2.5. FTIR (Fourier Transform Infrared) Analysis

For 6 hours, a mild steel coin was submerged in 1 M phosphoric acid containing 800 ppm extract. After 6 hours, the sample was retrieved, dried, and the film that had formed on the surface was gently removed and used.

for the purpose of FTIR analysis

3. DISCUSSION AND RESULTS

3.1. Experiments on weight loss

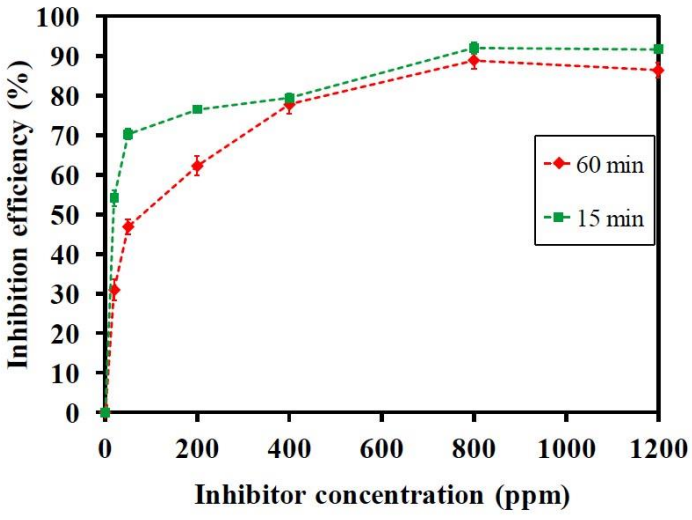

Figure 1 shows the effect of inhibitor concentration on mild steel inhibition in a 1 M phosphoric acid solution. (The line in the diagram serves as a visual aid; it does not indicate a data fit.) Figure 1 shows the inhibition efficiency of mild steel coupons immersed in 1 M phosphoric acid solution with various inhibitor concentrations. The 15-minute inhibition efficiencies Figure 1 depicts the 60-minute immersion time. Equation 1 [3] was used to compute the inhibitory efficiency.

$$\text{Inhibition efficiency \%} = \frac{W_0 - W_i}{W_0} \times 100$$

where W0 represents the weight loss of the coupons in the absence of the inhibitor, and Wi represents the weight loss of the coupons at a specific inhibitor concentration. Figure 1 shows that the inhibition efficacy improves with inhibitor concentration from 30% at 20 ppm to 80% at 60 min immersion duration.

At 800 ppm, it's 89 percent. For 1200 ppm extract, the inhibitory efficiency declines to 87 percent. The higher inhibition efficiency with increasing inhibitor concentration is thought to be owing to enhanced inhibitor molecule adsorption on the metal/solution interface with increasing inhibitor concentration [21]. The desorption of the inhibitor molecules back into the bulk when the concentration approaches the critical concentration may cause a modest decline in inhibition efficiency at 1200 ppm inhibitor concentration. The metal-inhibitor association is weakened by desorption, resulting in a reduction in inhibition efficacy [30, 35]. Figure 1 further shows that the inhibition effectiveness decreases with increased immersion time at lower inhibitor concentrations, however at higher concentrations, the variation in inhibition efficiencies with immersion time is not significant. In mild steel, the same trend has been observed.

In the presence of a cefazolin inhibitor, HCl was used [35].

3.2. Temperature's Influence

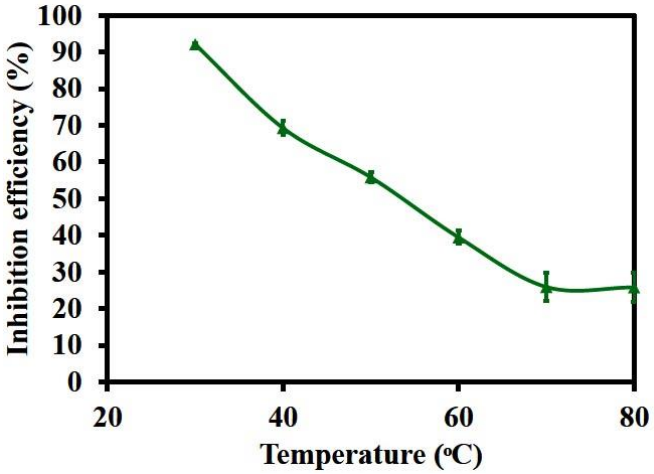

Figure 2: Inhibition efficacy of mild steel in 1 M phosphoric acid solution with 800 ppm inhibitor at various temperatures. (The line in the diagram serves as a visual aid; it does not indicate a data fit.)

In 1 M phosphoric acid, the influence of temperature on the corrosion rate (CR) of mild steel was investigated in the presence and absence of an inhibitor. The temperature range investigated was 30°C to 80°C. In the studies, the inhibitor concentration was 800 ppm.

Figure 2 shows the inhibitory efficiency at various temperatures in the presence of 800 ppm extract.

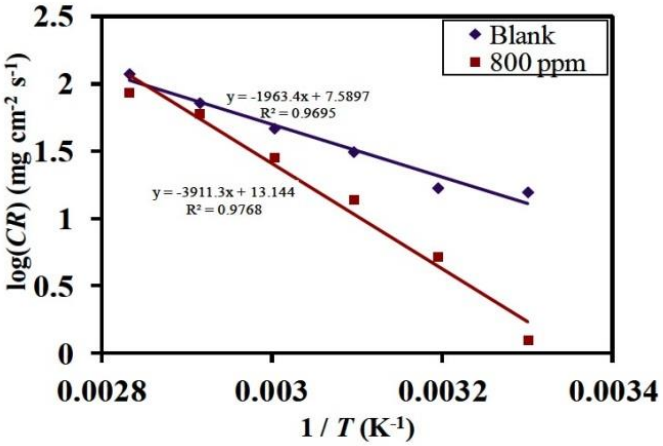

Figure 3: Arrhenius plots for mild steel in 1 M phosphoric acid with and without 800 ppm inhibitor in 1 M phosphoric acid solution.

Due to a decrease in hydrogen evolution over potential, mild steel dissolving in acidic media increases with increasing temperature [26]. This demonstrates that guava leaf extract can help to reduce corrosion at higher temperatures to some extent. The effectiveness of the inhibitor

As the temperature rises, the extract decreases. At 30°C, the inhibition efficiency was 92 percent, while at 80°C, it was just 27 percent. Increased dissolving of mild steel with higher temperatures, as well as desorption of the adsorbed inhibitor molecules from the metal, could explain the decrease in inhibitory efficiency.[27] surface

Using the Arrhenius equation, the activation energy (Ea) for the system in the presence and absence of inhibitor was computed. Weight loss measures yielded a log (CR) that was a linear function of temperature [27].

$$\text{Log (CR)} = -\frac{E_a}{2.303RT} + A$$

where Ea represents the apparent effective activation energy, R represents the gas constant, A represents the Arrhenius pre-exponential factor, and T represents the temperature. The Arrhenius plots for mild steel in 1 M phosphoric acid with and without 800 ppm inhibitor are shown in Figure 3. The Ea of the system was calculated to be 37 kJ mol-1 in the absence of inhibitor, and 75 kJ mol-1 with 800 ppm inhibitor. It's possible that the increased Ea with the addition of inhibitors is related to the increased energy barrier of the cell.Reaction to rusting [26]. Physical adsorption is thought to be the cause of the adsorptive film generated on the metal's surface when the inhibition efficacy decreases with rising temperature and the Ea in the presence of inhibitor is higher than the Ea in the absence of inhibitor [32]. Increased metal dissolution at higher temperatures and weakening of the physisorbed inhibitor layer at higher temperatures in the presence of inhibitor can also explain a decrease in inhibition efficiency [9].

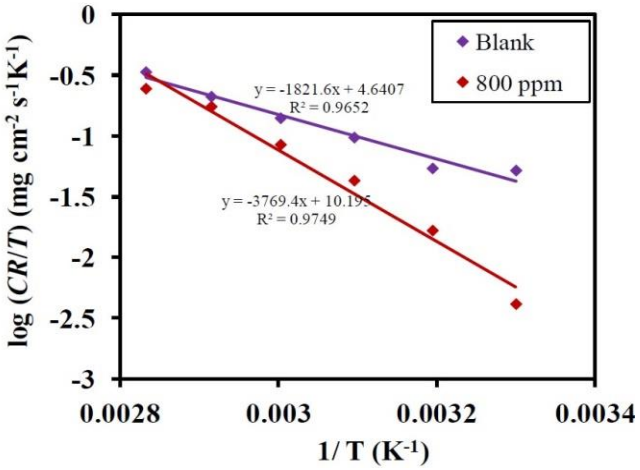

Figure 4: Plots of log (CR/T) vs. 1/T in 1 M phosphoric acid with and without 800 ppm inhibitor for mild steel in 1 M phosphoric acid. However, according to the literature, adsorption processes with Ea less than 40 kJ mol-1 are classified as physical adsorption, while those with Ea greater than 80 kJ mol-1 are classified as chemisorption. The guava leaf extract with an activation energy of 75 kJ mol-1 can be deduced from the preceding relationships.
complete adsorption [33-35], which is a mix of physical and chemical adsorption.
Due to competing adsorption with water molecules, the removal of which requires some activation energy, Ea is not a trustworthy metric for describing the nature of adsorption [36]. The enthalpy of activation (Ha) and entropy of activation (Sa) for the system were computed using the transition state equation 3 from the results of studies on weight loss at different temperatures with and without 800 ppm inhibitor [10, 11, 37] to further examine the system thermodynamics.

$$\text{Log}\left(\frac{CR}{T}\right) = \log\left(\frac{R}{Nh}\right) + \frac{\Delta S_a}{2.303R} - \frac{\Delta H_a}{2.303RT}$$

R stands for the universal gas constant, N for Avogadro's number, and h for Planck's constant. Figure 4 shows a straight line plot of log (CR/T) vs 1/T with a slope of Ha/2.303R and an intercept of log(R/Nh)+(Sa/2.303R). In the presence of Ha and Sa, their values
Table 1 shows the presence and absence of the 800 ppm inhibitor.

Table-1 shows the thermodynamic characteristics of mild steel in 1 M phosphoric acid with and without an inhibitor of 800 ppm.

	Inhibitor concentration mg L^{-1}	
Parameter	**0**	**800**
ΔH_a (kJ mol^{-1})	34	72
E_a (kJ mol^{-1})	37	75
ΔS_a (J $mol^{-1}K^{-1}$)	-108	-2

With the addition of the extract, the Ha rises. The results are consistent with those reported in the literature for mild steel in acidic medium, both with and without the inhibitor [10, 27]. A

positive value for Ha indicates that the dissolving process is endothermic and that the dissolution is taking place in the presence of an inhibitor.

At lower temperatures, more energy is required, resulting in improved inhibition efficiency. [10]

In both circumstances, ΔSa is negative, with the Sa value for the system without inhibitor being higher. A negative ΔSa indicates that the activation complex is in charge of the corrosion process [10]. A closer examination of the Sa values reveals that they are moving in a good manner.the extract's existence. The creation of the adsorbed layer on the metal surface, which is thought to increase the system's disorderliness, is responsible for such a positive change. The inhibitor layer prevents hydrogen ions from being liberated at the metal surface, resulting in enhanced disorderliness and system entropy [10, 38].

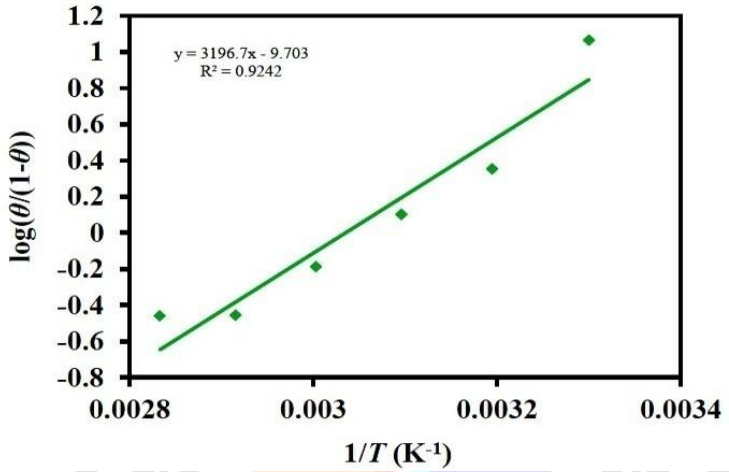

Figure 5 Plots of log (θ/(1-θ) vs. 1/T in 1 M phosphoric acid with 800 ppm inhibitor for mild steel.

The adsorption heat At constant pressure settings, Qads is equal to the enthalpy of adsorption (ΔHads) [39]. Equation 4 [39] was used to obtain the value of Qads for the system at a fixed inhibitor concentration.

$$\text{Log}\left(\frac{\theta}{1-\theta}\right) = logA + logC - \frac{Q_{ads}}{2.303RT} \qquad (4)$$

where is the inhibitor concentration, A is a constant, and C is the surface coverage.Using the surface coverage values for the system with 800 ppm extract in the temperature range from 30°C to 80°C a plot of log(θ/(1- θ)) vs. 1/T .

The straight line has a slope of -ΔHads/2.303R. ΔHads was calculated to have a value of -61.2 kJ mol-1. A negative ΔHads value indicates that the inhibitor molecule's adsorption on a mild steel surface is exothermic, and a negative ΔHads value can indicate either physisorption or chemisorptions process. An absolute Δ*H*ads value of 41.86 kJ mol-1 or lower is considered as Physisorption is defined as a value of 41.86 kJ mol-1 or less, while chemisorption is defined as a value more than 100 kJ mol-1 [35]. Because the current system produces a ΔHads of -61.2 kJ mol-1, it can be classified as a hybrid between chemical and physical adsorption in its whole [35-40].

3.3. Studies on potentiodynamic polarization

Figure 6 shows the results of potentiodynamic polarisation tests using mild steel as the working electrode in 1 M phosphoric acid at various inhibitor doses.
The corrosion current (Icorr) values computed from the Tafel plots using linear extrapolation are given in the graph.
Table No. 2

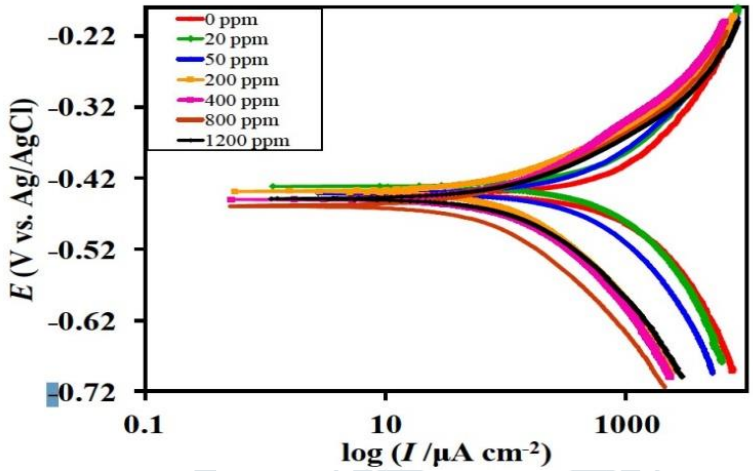

Figure 6. Potentiodynamic polarization plots for mild steel in 1 M phosphoric acid at various inhibitor concentrations. The scan rate used was 1 mV s-1.
Table 2. Tafel parameters and inhibition efficiency for mild steel in 1 M phosphoric acid at various inhibitor concentrations

Concentration (mg L^{-1})	E_{corr} (mV vs. Ag/ AgCl)	I_{corr} (µA cm^{-2})	β_c (mV dec^{-1})	β_a (mV dec^{-1})	Inhibition Efficiency %
0	-427	975	-256	204	0
20	-431	929	-260	229	5
50	-437	651	-255	192	33
200	-450	206	-205	131	79
400	-439	182	-214	127	81
800	-459	107	-178	104	89
1200	-456	252	-215	137	74

Equation 5 [27] was used to compute the inhibition efficiency from the Icorr data.

$$\text{Inhibition efficiency (\%)} = \frac{I^0_{corr} - I^i_{corr}}{I^0_{corr}} \times 100$$

In the preceding equation, I^o_{corr} corr represents the corrosion current in the absence of inhibitor, and I^i_{corr} represents the corrosion current in the presence of inhibitor.With any given inhibitor dosage, is the corrosion current The inclusion of the inhibitor reduces both cathodic hydrogen and anodic hydrogen, as shown in Figure 6.Anodic metal dissolution processes and development [39, 41, 42].

When the inhibitor concentration is increased to 800 ppm, the Icorr values decline dramatically, then marginally increase at 1200 ppm. With an increase in temperature, the corrosion potential values (Ecorr) demonstrate a change towards a greater negative potential.

Up to 800 ppm inhibitor concentration For 1200, the Ecorr value shifts slightly to the positive side.

ppm is a unit of measurement for the concentration of an extract.

Mixed type inhibitors cause a negative shift in the Ecorr readings after the addition of an inhibitor. 42, 41] Furthermore, research suggests that if the maximal displacement in the Ecorr is greater than 85 mV, the inhibitor is cathodic or anodic, and if it is less than 85 mV, the inhibitor is cathodic or anodic.

It is classified as a mixed type inhibitor if the voltage is more than 85 mV [24]. Ecorr's maximal displacement was calculated to be 28 mV vs. Ag/AgCl, indicating that the extract is a mixed type inhibitor. When the inhibitor is removed from the equation, the inhibition efficiency drops slightly.

The concentration was raised from 800 to 1200 parts per million. A similar trend was observed when the *Zenthoxylum alatum* plant extract was used as inhibitor for mild steel in 20% phosphoric acid. A drop in inhibition efficiency and an increase in *I*corr value were observed when the concentration was increased from 2400 ppm to 3200 ppm [33]. The desorption of molecules from the metal surface may cause a decrease in inhibition efficacy at higher inhibitor doses [36, 41, 42]. The cathodic current-potential curves at varied inhibitor doses may be seen in Figure.6.are in a straight line with each other. This demonstrates that the addition of an inhibitor has no effect on the mechanism of hydrogen evolution [36, 41, 42]. The charge transfer mechanism is responsible for the reduction of H+ ions at the mild steel surface [36]. It's also worth noting that the rate of metal breakdown is lower in the

Although there is an inhibitor present at low anodic over potentials, it increases significantly with larger anodic over potentials.potentials.

3.4 : Experiments with electrochemical impedance spectroscopy (EIS)

The Kramers Kronig Transformation (KKT) [43] can be used to verify the stability, causality, and linearity of impedance data from a system.The most useful forms of KKT are as follows[44]

$$Z^{''}(\omega) = \frac{2\omega}{\pi}\int_0^{\infty}\frac{Z^{'}(x) - Z^{'}(\omega)}{x^2 - \omega^2}\mathrm{dx} \qquad (6)$$

$$Z^{'}(\omega) = Z^{'}(\infty) + \frac{2}{\pi}\int_0^{\infty}\frac{xZ^{''}(x) - \omega Z^{''}(\omega)}{x^2 - \omega^2}\mathrm{dx} \qquad (7)$$

The real and imaginary impedance values are Z′ and Z″, respectively. The angular frequency can be determined using the formula $\omega = 2\pi$f, where f is the frequency in Hz. The impedance represented as a function of is called Z (↑ ω). The Z (ω) is used to compute the value of integrals in 6 and 7.

based on experimental data collected over a limited frequency range ($\omega_{min.}, \omega_{max.}$).

It is interpolated to assure sufficient integration accuracy with small integration steps dx and extrapolated to $\omega \rightarrow 0$ and to $\omega \rightarrow \infty$ [44].It can be seen from the plots that the experimental and the calculated values match well. The Nyquist plots for mild steel in 1 M phosphoric acid medium at varied inhibitor doses are shown in Figure 8. For all inhibitor doses, the Nyquist plot reveals a depressed.

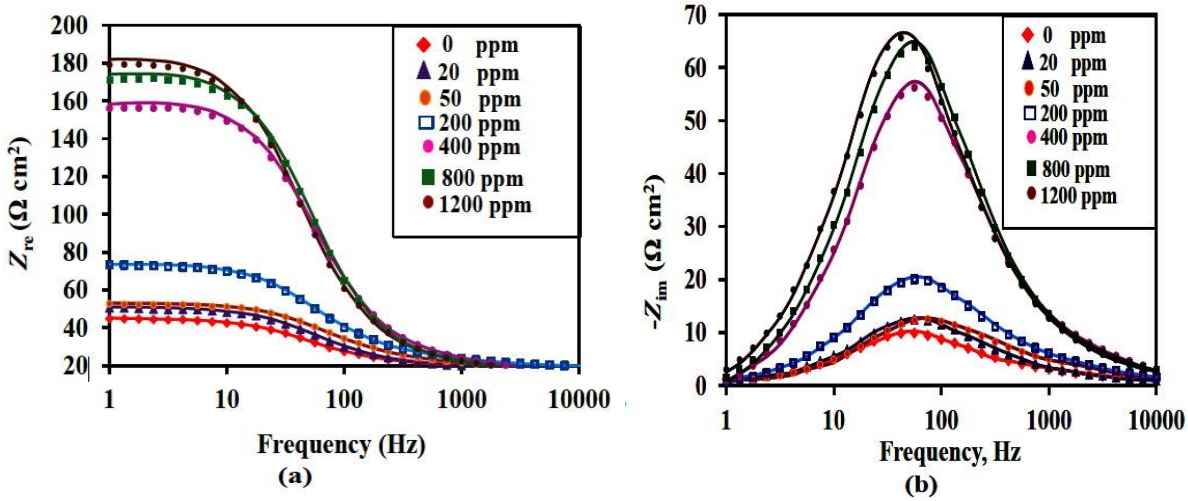

Figure 7. KKT fits for the EIS data for mild steel in 1 M phosphoric acid at various inhibitor concentrations. The solid lines represent the KKT fit. **(a)** KKT fits showing Zre vs. frequency **(b)**KKT fits showing -Zim vs. frequency

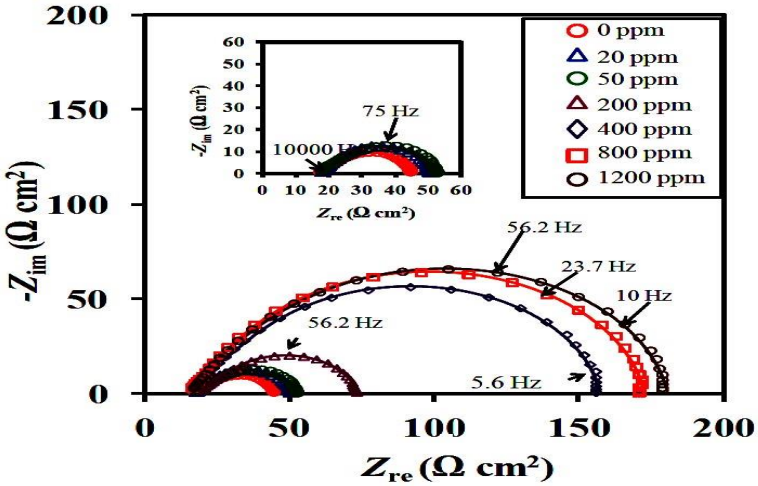

Figure 8: Nyquist plots in 1 M phosphoric acid for mild steel at various inhibitor doses at OCP. The Nyquist plots for inhibitor doses of 0,20, and 50 ppm are shown in the inset figure (the line denotes the EEC fit).

Frequency dispersion due to surface inhomogeneity or roughness is typically referred to as high frequency loops with a depressed semi-circular shape [26, 35**].** Furthermore, the impedance patterns demonstrate the creation of an arc in the low frequency end, which is attributed to the adsorbed species' relaxation process or the re-dissolution of the passivated surface at low frequencies.frequencies that are lower [26 and 35]. The Nyquist plots were modelled using an electrical equivalent circuit (EEC) consisting of three resistances and two constant phase elements (CPE) that has been used to mimic a variety of dissolving systems [8, 43, 45]. The appearance of a depressed semicircle is due to the metal electrode's non-uniformity and surface roughness,[35], hence CPEs were utilised instead of perfect capacitors. A parallel combination of a pure capacitor and a resistor is referred to as a CPE. The angular frequency is inversely proportional [26]. The metal-solution interface is thought to operate as a capacitor with irregular surface when the impedance pattern has a depressed semicircle, as indicated by CPE [26]. The mathematical expression defines a CPE.Equation 8 [26] provides the answer

$$Z_{cep} = \frac{1}{Y_{0[J\omega]^n}}$$

*Z*CPE in equation is the impedance of CPE, ***Y0*** is the proportionality constant, ω is the angular frequency and *n* is the surface roughness parameter [26, 43, 44].

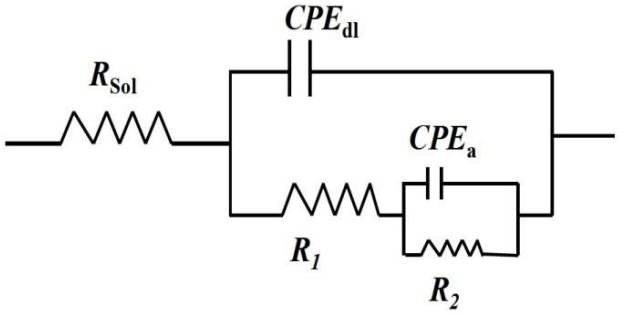

Figure 9 shows the electrical equivalent circuit (EEC) for 1 M phosphoric acid with different inhibitor concentrations**.**

Figure 9 depicts the comparable circuit. Rsol is the system's solution resistance, R1 is the charge transfer resistance for the corrosion reaction, and R2 is the double layer resistance. CPEdl denotes the capacitance of the electrical double layer at the metal-solution interface, while R2 and CPEa denote the adsorbed layer's pseudo resistance and capacitance [8, 43, 45, 46]. A combination of negative and positive frequencies is used to explain the creation of a tiny arc at the lower frequency end.The terms "resistance" and "CPE" are employed. Because it is difficult to convey a physical viewpoint to employ a large inductance, this combination is often used to portray arcs with inductive behaviour [26]. Using equation 9 [46], the double layer capacitance (Cdl) was calculated from the CPE parameters.

$$\boldsymbol{C_{di} = (y_d R^{1-n_d}) \frac{1}{nd}}$$

The relaxation time constant (τd) of charge transfer process was calculated using equation 10 [46]

$$\tau_d = C_{dl}\, R_1$$

Similarly the relaxation time constant (τa) for the adsorption process was calculated using equation 11.

Table 3. EEC fit parameters with relaxation time constants

Con. (mg L^{-1})	R_{sol} (Ω cm^2)	Y_d (10^5 Ω^{-1} $s^n cm^{-2}$)	n_d	R_1 (Ω cm^2)	C_{dl} (μF cm^{-2})	τ_d (10^4s)	Y_a (10^5 Ω^{-1} $s^n cm^{-2}$)	n_a	R_a (Ω cm^2)	C_a (μFcm^{-2})	τ_a (10^3s)	*IE* %
0	17.1	2	0.77	9.7	31	3	10	0.93	18.3	62	1	-
20	17.7	7	0.87	6.8	22	1.5	10	0.84	26.3	32	1	15
50	17.4	6	0.85	10.7	16	1.8	10	0.86	24.81	38	1	21
200	19.4	4	0.86	13.2	12	1.5	9	0.86	41.2	36	1.4	49
400	17.1	1	0.93	36.2	11	2	3	0.89	104.2	15	1.5	80
800	16.4	2	0.93	41.3	12	4.8	2	0.88	115	9	1	82
1200	17.4	2	0.92	61.6	11	6.9	3	0.9	101.8	1.6	1.6	82

The Cdl values fall as inhibitor concentrations rise, which could be attributed to inhibitor molecules forming a protective layer [46]. The decrease in surface inhomogeneity due to the rise in inhibitor concentration could explain the increase in nd values. Inhibitor compounds

that have been adsorbed [46]. With increasing inhibitor concentration, an increased nd value also indicates a decrease in charge and discharge rates [46]. The energy dissipation within the adsorbed layer explains why the values of na are smaller than those of nd [46]. Similarly With a rise in inhibitor concentration, Ca values decrease. This could be due to inhibitor molecules adsorbing to the surface, lowering the local dielectric constant [12,29,30]. Ra is the most powerful player in the Rp. With increasing inhibitor concentrations up to 800 ppm, the inhibition efficiency improves At 1200 ppm, it saturates. The EIS results yielded a maximum efficiency of 82 percent.

3.5. Adsorption isotherm

The inhibitor molecules' adsorption on the metal surface is thought to coincide with the desorption of water molecules at the metal surface, resulting in an exchange mechanism [29, 40-42]. With increasing inhibitor concentrationsAt various doses of inhibitor, weight loss measurements, potentiodynamic polarisation, and electrochemical impedance spectroscopy demonstrate improved inhibition efficacy. The inhibitor bonds to the metal surface, as evidenced by this. that the surface covering increases as the inhibitor concentration rises. Langmuir and Temkin were used to analyse the data.isotherm of adsorption Equation 13 [10] .

$$\theta = \frac{-lnk_{ads}}{2a} - \frac{\ln c}{2a}$$

The adsorption equilibrium constant is k ads, and the attractive parameter is an in the preceding equation.

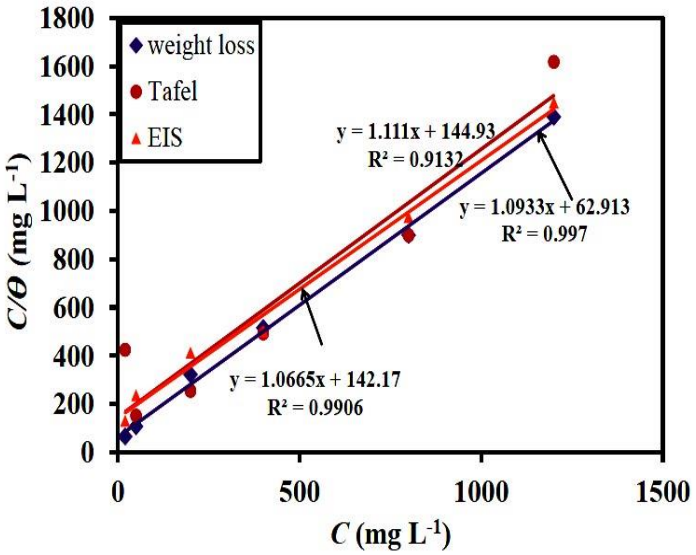

Figure 10. Langmuir adsorption isotherms for mild steel in 1 M phosphoric acid with and without 800 ppm inhibitor.

the Temkin isotherm equation's outcomes The equation is used to compute the standard free energy of adsorption …….. (1)

$$\Delta G^0_{ads} = -RTln\,(k_{ads} \times p_w)$$

where *R* is universal gas constant, *T* is the absolute temperature in Kelvin, ρW is the density of water in g L-1. The values of *k*ads and Δ*G*°ads for both Langmuir and Temkin isotherms calculated using the equations 13, 14 and 15 are listed in the Table 4

Table 4. Langmuir adsorption isotherm parameters for mild steel in 1 M phosphoric acid with and without 800 ppm inhibitor

Parameter	Weight loss	Tafel	EIS
Langmuir			
k_{ads} (L g^{-1})	7.03	15.7	16.5
ΔG^0_{ads} (kJ mol^{-1})	-41	-39	-39
Temkin			
$\ln k_{ads}$ (L g^{-1})	6	4	4
ΔG^0_{ads} (kJ mol^{-1})	-33	-29	-28

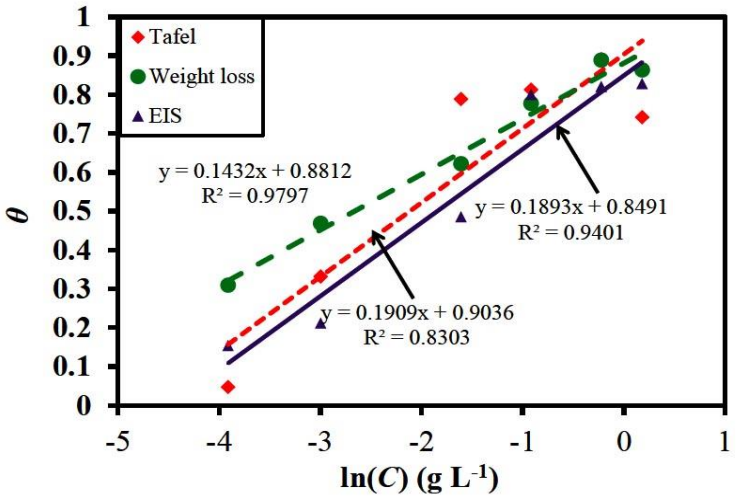

Figure 11. Mild steel Temkin adsorption isotherms in 1 M phosphoric acid with and without 800 ppm inhibitor.

The adsorption process is spontaneous, as evidenced by the negative values of G° ads. G° is a number with a value of 1.

For the Langmuir adsorption isotherm, ads ranges between -39 kJ mol-1 and -41 kJ mol-1. The Temkin is a character in the novel The Temkin ΔG° is the result of the isotherm.A ΔG° has values ranging from -28 kJ mol-1 to -39 kJ mol-1.− 40 kJ mol-1 is the advertised value.Between chemical and physical adsorption methods, the threshold value was studied [39-42]. Physisorption is represented by values up to -20 kJ mol-1, while chemisorption is represented by values more negative than – 40 kJ mol-1 [39-42]. Thus, the G°ads values for the current system are in the intermediate range, implying a thorough adsorption involving both physical and chemical adsorption, with chemisorption dominating.

3.6. Scanning electron microscopy

Figure 11….

When comparing the surface of the sample immersed in phosphoric acid solution in the absence of inhibitor to the sample kept in the presence of inhibitor, it is obvious that the surface of the sample immersed in phosphoric acid solution in the presence of inhibitor displays substantial corrosion.

3.7. FTIR analysis

The peaks from FTIR analysis of the sample obtained from mild steel coupons immersed in 1 M phosphoric acid solution containing 800 ppm extract are shown in Table 5

Table 5. Peak locations in the FTIR spectrum for a mild steel sample immersed in 1 M phosphoric acid with 800 ppm inhibitor.

Frequency cm^{-1}	Band assignment
792	Iron oxide
1007	Iron phosphate complex
1250	-C-C stretch
1559.6	COO^- stretch
1620	Iron phosphate
2364.7	N-H stretching vibration
2981	-CH stretch
3100	N-H stretch
3674	OH stretching vibration
3838.1	OH stretching vibration

Iron phosphate is seen in the bands at 1007 cm-1 and 1620 cm-1, while iron oxide is present in the band at 792 cm-1 [33]. The adsorption of plant extract molecules on mild steel surface could explain the bands at 1250 cm-1, 3100 cm-1, 2364.7 cm-1, and 2981 cm-1 [47].

3.8. Mechanism

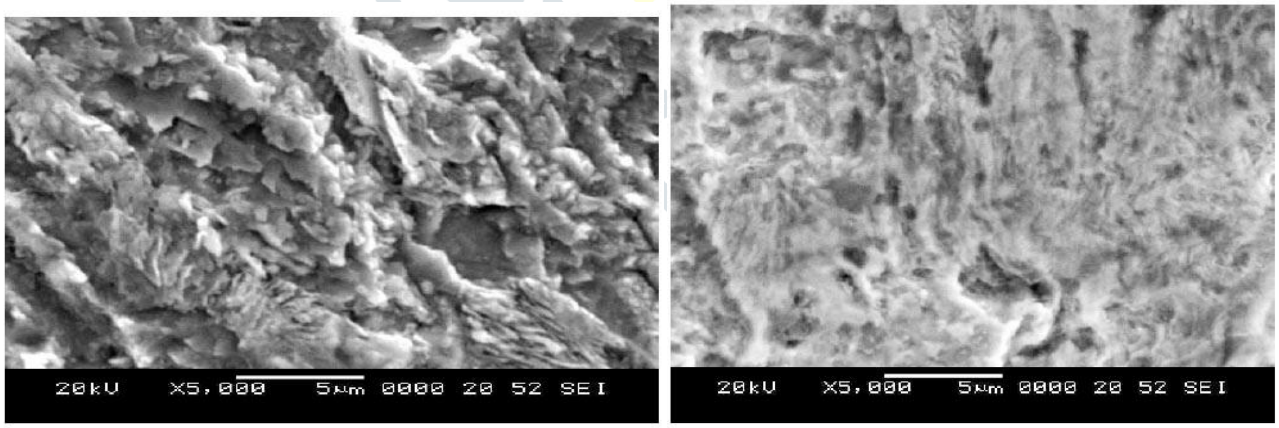

a b

Figure 12. Scanning electron micrographs of mild steel immersed in 1 M phosphoric acid for 6 hours (a) without and (b) with 800 ppm inhibitor.

A mechanism for corrosion inhibition can be hypothesised based on the above-mentioned discussions. The plant extract molecules are thought to have been present in the phosphoric acid solution at first. The production of Fe2+ is caused by the dissolving

of mild steel in the early phases. The plant extract reacts with the Fe2+ ions and forms organo-metal complex (Fe-E) which forms .

4. CONCLUSIONS

- In a 1 M phosphoric acid media, A mild steel corrosion inhibitor was discovered to be an alcoholic extract of Pisidium guajava (Guava) leaves. In weight loss trials with a 1 h immersion time, an inhibitor concentration of 800 ppm resulted in a maximum inhibition efficiency of 89 percent.
- the inhibition efficiency decreased with increasing temperature and the apparent activation energy increased to 75 kJ mol-1 from 37.5 kJ mol-1, indicating that the corrosion reaction energy barrier is increased with the addition of inhibitor and the activation energy is in the range of comprehensive adsorption.
- Langmuir and Temkin adsorption isotherms were used to analyse the system, yielding G°ads values ranging from -28 to -41 kJ mol-1 and a heat of adsorption value of -61.2 kJ mol-1, showing that the adsorption is of the intermediate type, mixing physical and chemical adsorption.

ACKNOWLEDGEMENTS

Prof. S. Ramanathan of IIT-Madras graciously granted permission to conduct electrochemical experiments to the writers.

1. R.M. Silverstein, F.X. Webster, D.J. Kiemle, *Spectrometric Identification of Organic Compounds*, John Wiley and Sons, USA (2005) p. 101.
2. M. Tourabi, K. Nohair, M. Traisnel, C. Jama, F. Bentiss, *Corros. Sci*., 75 (2013) 123.
3. R. Sabino, B.S. Azambuja, R.S. Gonçalves, *J. Solid State Electrochem.*, 14, (2010) 1255.
4. X. Li, G. Mu, *Appl. Surf. Sci*., 252 (2005) 1254.
5. R. Solmaz, *Corros. Sci*., 81 (2014) 4.
6. R. Solmaz, *Corros. Sci.*, 52 (2010) 3321.
7. R.P. Venkatesh, B. Jun Cho, S. Ramanathan, Jin-Goo Park, *J. Electrochem. Soc*., 159 (2012) C447.
8. A. Sadkowski, *Solid State Ionics*, 176 (2005) 1987.
9. A.K. Singh, M.A. Quraishi, *Corros. Sci*., 52 (2010) 152.
10. R. Solmaz, *Corros. Sci*., 79 (2014) 169.
11. M. Bouklah, B. Hammouti, M. Lagren'ee, F. Bentiss, *Corros. Sci*., 48 (2006) 2831.
12. K.M. Ismail, *Electrochim. Acta*, 52 (2007) 7811.
13. R. Solmaz, G. Kardas, B. Yazici, M. Erbil, *Colloids Surf. A*, 312 (2008) 7.
14. L.Y.S. Helen, A.A. Rahim, B. Saad, M.I. Saleh, P.B. Raja, *Int. J. Electrochem. Sci.*, 9 (2014) 830.
15. A.S. Yaro, A.A. Khadom, K.R. Wael, *Alexandria. Eng. J.*, 52 (2012) 129.
16. R.O. Ramos, A. Battistin, R.S. Gonçalves, *J. Solid State Electrochem.*, 16 (2012) 747.
17. D.M.O. Sotelo, J.G.G. Rodriguez, M.A.N. Flores, M. Casales, L. Martinez, A.V. Martinez, *J. Solid State Electrochem.*, 15 (2011) 997.

18. M. Abdeli , N.P. Ahmadi, R.A. Khosroshahi, *J. Solid State Electrochem*., 15 (2011) 867.
19. S.K. Shukla, E.E. Ebenso, *Int. J. Electrochem. Sci*., 6 (2011).
20. M. Abdeli , N.P. Ahmadi , R.A. Khosroshahi, *J. Solid State Electrochem*., 14 (2010) 1317.
21. P.C. Okafor, C.B. Liu, X. Liu, Y.G. Zheng, F. Wang, C.Y. Liu, F. Wang, *J. Solid State Electrochem*., 14 (2010) 1367.
22. I. Ahamad, R. Prasad, M.A. Quraishi, *J. Solid State Electrochem*., 14 (2010) 2095.
23. I. Ahamad, R. Prasad, M.A. Quraishi, *Corros. Sci*., 52 (2010) 933.
24. N.O. Eddy, E.E. Ebenso, U.J. Ibok, *J. Argent. Chem. Soc*., 97 (2009) 178.
25. F.S. De Souza, A. Spinelli, *Corros. Sci*., 51 (2009) 642.
26. K.F. Khaled, *J. Solid State Electrochem*., 13 (2009) 1743.
27. P.C. Okafor, E.E. Ebenso, U.J.Ekpe, *Int. J. Electrochem. Sci*., 5 (2010) 978.
28. M.A. Quraishi, A. Singh, V.K. Singh, D.K. Yadav, A.K. Singh, *Mater. Chem. Phys*., 122 (2010) 114.
29. A.K. Satapathy, G. Gunasekaran, S.C. Sahoo, K. Amit, P.V. Rodrigues, *Corros. Sci*., 51 (2009) 2848.
30. P.C. Okafor, M.E. Ikpi, I.E. Uwah, E.E. Ebenso, U.J. Ekpe, S.A. Umoren, *Corros. Sci*., 50 (2008) 2310.
31. E.E. Oguzie, *Corros. Sci*., 50 (2008) 2993.
32. G. Gunasekaran, L.R. Chauhan, *Electrochim. Acta*., 49 (2004) 4387.
33. M.S.S. Morad, A. El-Hagag, A. Hermas, M.A.S. Aal, *J. Chem. Technol. Biotechnol*., 77 (2002) 486.
34. S. Deng, X. Li, *Corros. Sci*., 55 (2012) 407.
35. M.H. Hussin, M.J. Kassim, N.N. Razali, N.H. Dahon, D. Nasshorudin, *Arabian J. Chem*., DOI: 10.1016/j.arabjc.2011.07.002 (2011).

.